THE PUBLISHING HOUSE
OF THE ROMANIAN ACADEMY

PROCEEDINGS OF THE ROMANIAN ACADEMY, Series A,
Volume 10, Number 1/2009, pp. 000–000

ELECTRONIC DEVICES BASED ON CARBON NANOTUBES AND GRAPHENE

Mircea DRAGOMAN

National Research and Development Institute in Microtechnology, Str. Erou Iancu Nicolae 32B, 077190 Bucharest, Romania
Email: mircea.dragoman@imt.ro

The electronic devices based on carbon nanotubes and graphene are the most advanced circuits in the area of nanoelectronics developed in the last years. The paper presents a brief review of the results obtained in the last years.

Keywords: Carbon nanotubes; graphene; nanoelectronics.

1. INTRODUCTION

The carbon nanotubes (CNTs) and graphene electronic devices are very attractive in the area of communications, sensing and biology due to amazing properties like the highest mobility ever measured in a solid, the higher Young modulus ever known, or the easy functionalization with various anaorganic or organic materials [1]. In the Table I the basic properties of nanotubes and graphene are summarized.

Parameter	*Value and units*	*Observations*
Length of the unit vector	2.49 Å	1.44 Å is the carbon bond length
Current density	>109 A/cm^2	-1000 times larger than the current density in copper - Measured in MWCNTs
Thermal conductivity	6600 W/mK	More thermally conductive than most crystals
Young modulus	1 TPa	Many orders of magnitude stronger than the steel
Mobility	10000-50000 cm^{2}V^{-1}s^{-1}	mobility around 100 000 cm^{2}V^{-1}s^{-1} (in suspended CNT) and 200 000 cm^{2}V^{-1}s^{-1} in suspended graphene
Mean free path (ballistic transport)	300-700 nm semiconducting CNT 1000-3000 nm metallic CNT	- Measured at room temperature - At least three time larger than the best semiconducting heterostructures
Conductance in ballistic transport	G=4e^2/h=155μS	R=1/G=6.5kΩ
Luttinger parameter *g*	0.22	The electrons are strongly correlated in CNTs
Orbital magnetic moment	0.7 meVT^{-1} (*d* = 2.6 nm) 1.5 meVT^{-1} (*d* = 5 nm)	The orbital magnetic moment depends on the tube diameter

There are some important categories of electronic devices based on CNT or graphene. First, nanoelectromechanical systems (NEMS) are simple mechanical systems such cantilevers, and double-clamped beams having at least one dimension of the order of few nanometers and which are electrostatically actuated by an external electrode. NEMS displays mechanical resonance frequencies in the range 100 MHz-5

GHz, so coinciding with the electromagnetic microwave spectrum [2]. NEMS have also very high mechanical quality factors of $10^2 – 10^3$ at room temperature, in the GHz range.

The correspondence between the electromagnetic GHz spectrum and NEMS mechanical frequency oscillations can be used for new innovative devices in the area of high frequency NEMS [3]. Further, we will demonstrate that simple NEMS configurations based on carbon nanotubes (CNTs) have important applications for signal processing in the GHz range. Other categories of CNT or graphene devices are transistors, switches, sensors such as gas sensors or harvesting devices able to collect energy from the sun or ambient electromagnetic environment.

2. MICROWAVE RESONATOR BASED ON AN ARRAY OF FEW MILLIONS OF CARBON NANOTUBES

When microwave signal frequencies are tuned near the mechanical resonant frequency of an array of metallic cantilevered carbon nanotubes (CNTs) sandwiched between two coplanar waveguide (CPW) lines (see Fig. 1 a), the CNTs array displays a notch in the microwave transmission coefficient due to a metal-dielectric transition of the carbon nanotube array at the mechanical resonant frequency of the cantilever. Thus, the CNTs array acts like a resonator. We have used a CNT array having 10^9 CNTs/cm^2.The measured quality factor of such an array of millions of CNTs cantilevers has a quality factor of 800 at room temperature at the fundamental resonance frequency of 1.4 GHz (see Fig. 1b) [4].

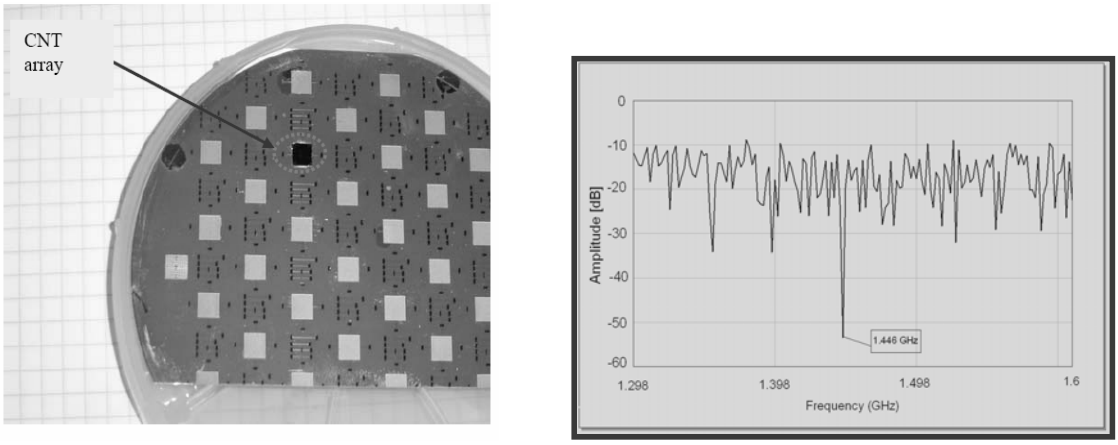

(a) (b)

Fig. 1 The CNT resonator. (a) The CNT array on the wafer and (b) the $|S_{21}|$ dependence on frequency

3. OSCILLATIONS AND AMPLIFICATION WITH SUSPENDED NANOTUBES

In what follows we present a double-clamped CNT bundle suspended over a metallized trench which is 1 μm wide and micromachined in GaAs substrate. In this configuration, this NEMS is behaving as FET-like device (see Fig.2, and 3). The drain and source contacts are made on the each side of the trench, while the gate is the metallized electrode of the gate located at 1.5 μm below the CNT bundle. The device is biased as FET transistor and low V_G is acting as variable resistor controlled by gate as any FET, but at certain gate voltage in the range 15-18 V, this structure displays a S shaped negative –differential resistance (NDR). Further, applying equal V_{DS} steps of 0.2 V the NDR is displaying multiple branches, which are parallel between them. In this way, the entire structure is working as a high speed switch with multiple levels which are very useful for multi-valued logic applications.

The I_D–V_D curve displayed in Fig. 4 shows that at low drain-source voltages V_D and for low gate voltages V_G the device is FET-like, i.e. a tunable resistor controlled by the gate voltage. However,, at higher voltages, i.e. for $V_D > 18$ V and $V_G > 12$ V, the I_D–V_D characteristics considerably changes, and shows a

multiple NDR behavior, as shown in Fig. 5. An S-shaped characteristics appears initially and then, at constant V_D steps of 0.2 V, the upper branch of the NDR is jumping and produces almost parallel 5–8 branches, depending on the V_D value.

The jumps in the I_D–V_D characteristics are most probably due to charge accumulation followed by potential lowering at the potential step discontinuities between different CNTs in the bundle. A similar mechanism has been evidenced in [5]. After overcoming the potential barrier at the electrode–CNT interface, which is responsible for the initial low-current region, the electrons in the CNT that is in direct contact with the electrode must overcome a potential barrier in order to penetrate in an adjacent CNT in the bundle (the potential barrier between adjacent CNTs is about 50 meV in height and 4 Å in width [6]). Charge accumulation at this potential barrier and the subsequent potential lowering, i.e. the jump in the I_D–V_D curve, means that electron transport is producing through another conduction channel/CNT each time such a jump is observed.

The traversal time τ of electrons across the potential barrier between adjacent CNTs was estimated at 10 fs and represents the switching time between two consecutive branches of the NDR characteristic. This signifies that our device is an ultrafast electric switch. This traversal time was calculated as $\tau = \int dx / v_g$, where the group velocity of electrons in the x direction (across the barrier) is defined as $v_g = J / |\Psi(x)|^2$, with $\Psi(x)$ the electron wavefunction in the barrier region and J the probability current.

The microwave measurements of our device were performed using a vector network analyzer (VNA) and a probe station. The probe-tip test structure connected to the FET-like architecture of our device is displayed in Fig. 6a. The maximum stable gain MSG = $|S_{21}|/|S_{12}|$ of a CNT-FET structure is shown in Fig. 6b for V_D = 1.6 V, V_G = 8 V and I_D = 2.25 mA. The measurements were performed in air and at room temperature. Microwave "on wafer" measurements were made using an Anritsu 37397D Network Analyzer in the 0.04–4 GHz range, a SOLT calibration procedure and the Picoprobe Calibration Substrate. The response includes the parasitics of the test structure. The results show that the active behavior of the CNT-FET structure is up to 3.25 GHz. The fact that S_{21} differs from S_{12} reveals the unilateral behavior of the device. Similar results were reported in [7], but at a much lower frequency (below 80 MHz). This device needs further matching networks and a minimization of parasitic capacitances in order to amplify in microwaves.

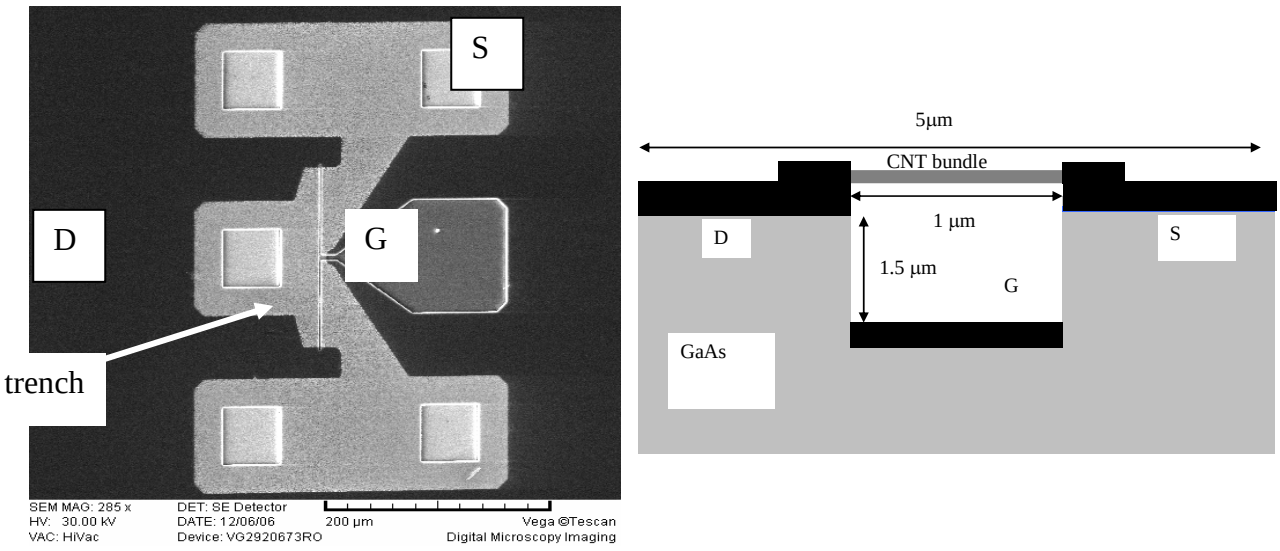

Fig. 2 The double clamped CNT bundle FET-like device

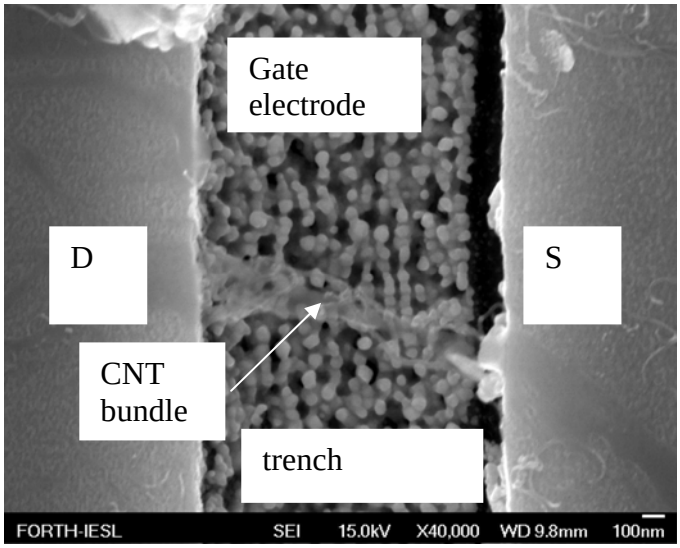

Fig. 3 The detail of the above device to evidence the CNT bundle

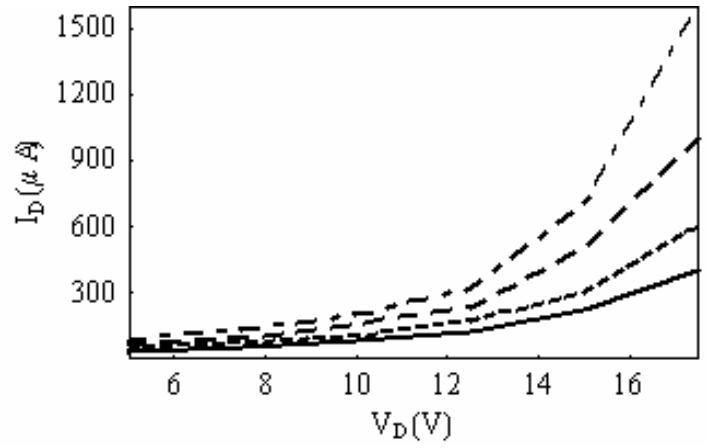

Fig. 4. The I_D–V_D dependence on the gate voltage for V_G = 0 (solid line), 4 V (dotted line), 8 V (dashed line), and 12 V (dashed-dotted line)

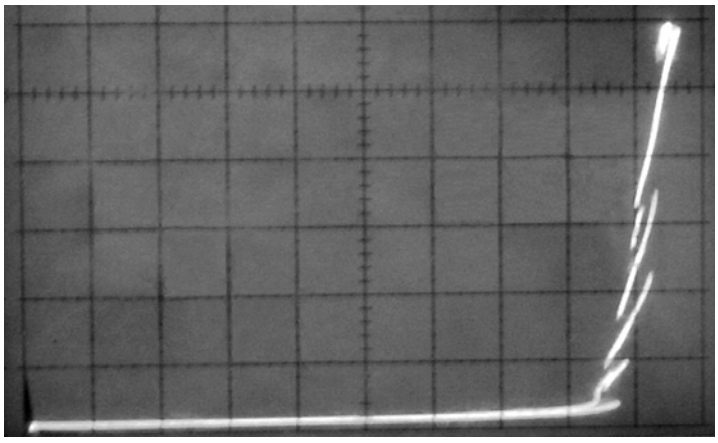

Fig. 5 Multiple NDR of the device (V_G =14 V; I_D -500μA/div and V_D -2V/div)

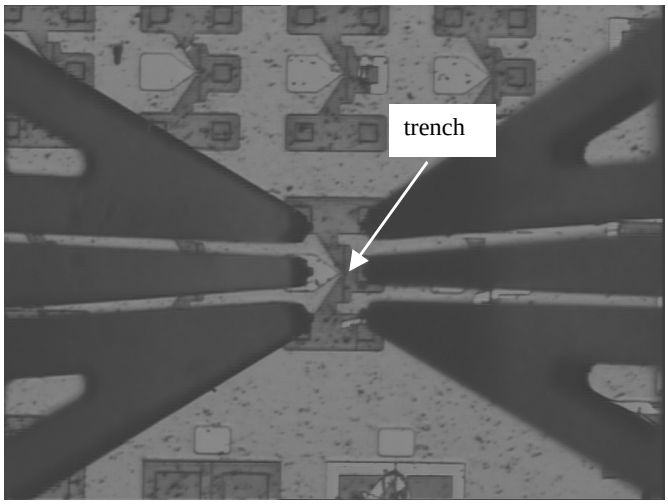

(a)

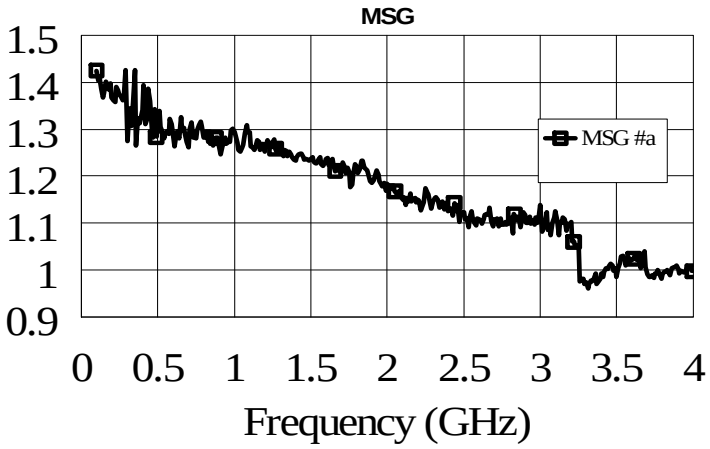

(b)

Fig. 6 (a) The probe-tip mounted on the CNT FET-like structure, and (b) the MSG characteristics

4. RF GRAPHENE DEVICES

Graphene is a native one-atom-thick crystal consisting of a single sheet of carbon atoms. In this material, discovered in 2005, the electron transport is ballistic at room temperature and is described by a relativistic-like quantum Dirac equation instead of a Schrödinger equation [8]. Also, graphene has a Young modulus of 1.5 TPa. Due to these unique properties, graphene is very promising for high frequency nanoelectronic devices, such as oscillators and switches working at high frequencies..We will demonstrate that graphene is a very efficient RF switch for microwave applications , tuning its resistivity from high values to low values with the help of a gate voltage. The switch is formed by a metallic CPW patterned over a graphene sheet grown over 300 nm of SiO_2. The SiO_2 is grown on a doped Si substrate playing the role of the gate. The results of the simulations are displayed in Fig.7. The switching characteristics are also evidenced in the current distribution at 60 GHz displayed in Fig. 8.

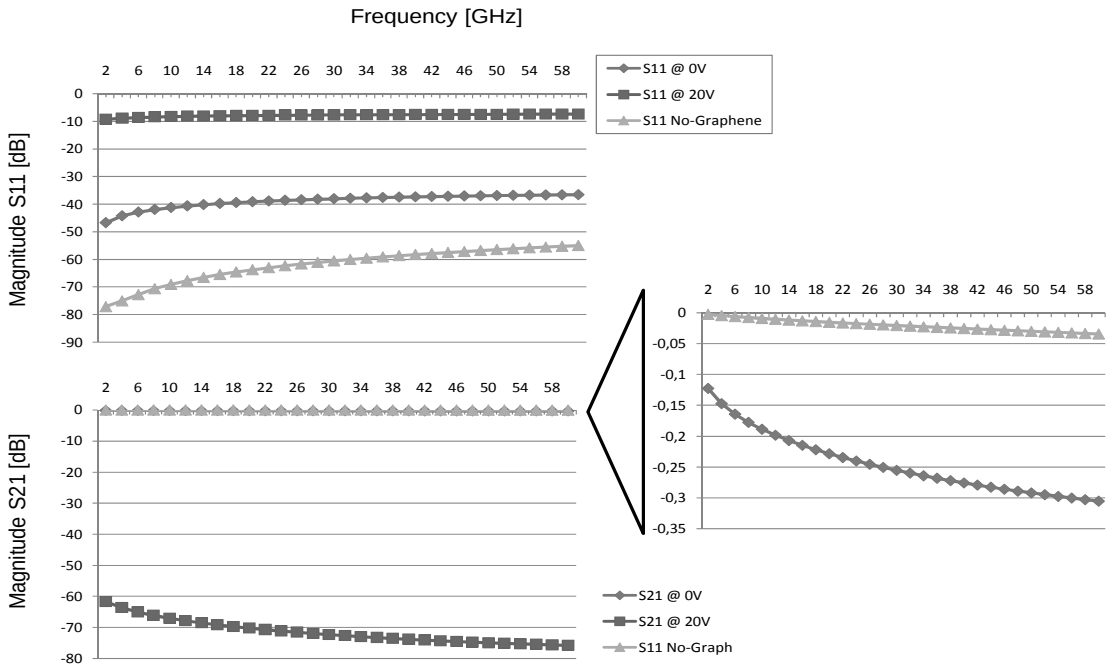

Fig. 7 Graphene switch up to 60 GHz

Fig. 8 The current distribution of CPW patterned over a graphene sheet when the gate voltage is tuned in the range 0-15 V.

Very recently, we have demonstrated that a graphene barrier dispays a pronounced negative differential resistanace (NDR)at room temperature [9]. NDR is the key element of the majority of oscillators and because in graphene the transport is ballistic it is expected that terahertz (THz) oscillators could be implemented based on graphene.In semiconductor heterostructures the transmission through a barrier is decaying exponentially with the barrier width and height, because inside the barrier the wavenumber is purely imaginary and corresponds to an evanescent propagation. The transmission can equal 1 only in the particular

case of resonant tunnelling heterostructures which have very important applications in high-speed devices such as resonant tunnelling diodes and semiconductor cascade lasers.

Klein tunnelling mechanism is proposed to express the tunnelling effect in graphene because the Dirac equation is describing the transport of massless fermions. In graphene, Klein paradox tell us that in deep contrast with semiconductor heterostructures, if the ballistic electrons are normally incident on the barrier, the transmission is 1 irrespective of the barrier height and width since electron propagation is not evanescent inside the barrier region. This is happens because the holes take the role of electrons as charge carriers in barriers. Thus, a single graphene barrier is equivalent to resonant tunnelling based on common semiconductor heterostructures and thus displays a NDR, like any resonant tunnelling structure. The transmission of the graphene barrier is represented in Fig. 9 as a function of applied dc voltage and at various Fermi wavenumbers $k_F = \alpha k_{F0}$, where α is 0.25, 0.3 and 0.35 when the inclination angle of the electron wavefunction is $\varphi = 15^0$ and the barrier width is $W = 100$ nm, where k_{F0}=50 nm. The main feature in Fig. 9 is a wide gap the transmission, which increases when k_F is increasing. This happens because the transmission of the incident wavefunction is forbidden in the barrier because otherwise the wavenumber inside the barrier will be imaginary, and this is not allowed by the gapless band energy diagram of the graphene. So, the graphene is a native quantum switch. Such an abrupt ON-OFF characteristic is among the best known in nanoelectronic devices.

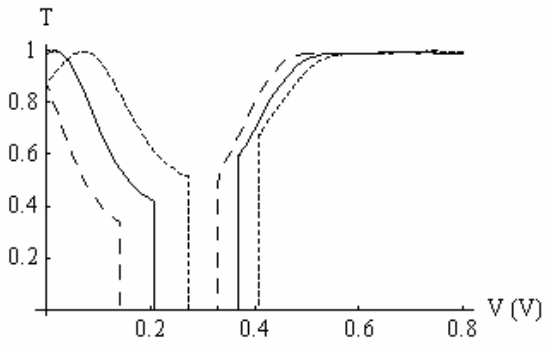

Fig. 9 Transmission of the graphene barrier as a function of the applied voltage at various Fermi wavenumbers: $k_F = 0.25\ k_{F0}$ (dotted line), $k_F = 0.3\ k_{F0}$ (solid line), and $k_F = 0.35\ k_{F0}$ (dashed line).

The corresponding current-voltage dependence was computed using Landauer and it is displayed in Fig. 10.

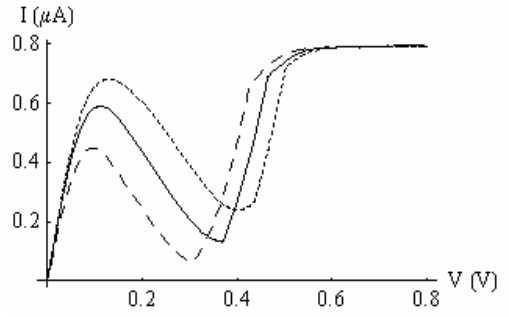

Fig.10 The *I-V* characteristics of graphene barrier at various Fermi wave numbers: $k_F = 0.25\ k_{F0}$ (dotted line), $k_F = 0.3\ k_{F0}$ (solid line), and $k_F = 0.35\ k_{F0}$ (dashed line).

The NDR region in graphene is due to the gap in the transmission characteristics while in a resonant tunnelling diode based on semiconductor heterostructures the NDR is originating from a narrow peak in the transmission.

Other graphene devices were recently reported such as nonvolatile switches [10] or field-effect transistors [11].

CONCLUSIONS

The new materials originating from the accelerated development of the nanotechnologies and nanoelectronics have a large impact in the RF devices conferring them miniaturization, reconfigurability, and new functionalities.

ACKNODLEGEMENTS

The author wish to thank many people helping him in the quest in the area of nanoelectronics, most of them being co-authors of many papers published in the last period of time. My wife Daniela has helped me with her deep knowledge in the area of quantum mechanics and solid state. My colleagues from IMT Bucharest and dr.George Konstantinidis from FORTH Heraklion, Greece, were behind almost any device reported in this paper especially due to their invaluable knowledge in the area of semiconductor technology. Prof. Dan Dascalu and Prof. Robert Plana are general managers and scientists with a very advanced vision about nanotechnology and they encouraged me always in my researches to go further. I also am indebt Prof. Hans Hartnagel who during many years has helped and guided me in the area of nanoelectronics.

REFERENCES

1. DRAGOMAN, M., DRAGOMAN, D., *Nanoelectronics: Principles and Devices*, Boston, Artech House, 2006.
2. EKINCI, K.L., ROUKES, M.L., *Nanoelectromechanical systems*, Rev. Sci. Instr., **76**, pp. 061101/1-4, 2005.
3. PENG, H.B., CHANG, C.W., ALONI, S., YUZVINSKY, T.D., ZETTL, A., *Ultrahigh frequency nanotube resonators*, Phys. Rev. Lett., **97**, pp. 087203/1-4, 2006.
4. DRAGOMAN, M., NECULOIU, D., CISMARU, A., GRENIER, K., PACCHINI, S., MASENQ, L., PLANA, R., *High quality nanoelectromechanical microwave resonator based on a carbon nanotube array*, Appl. Phys. Lett., **92**, pp. 063118/1-3, 2008.
5. LIU, W.-C., LAIH, L.-W., CHENG, S.-Y., CHANG, W.-L., WANG, W.-C., CHEN, J.-Y., LIN, P.-H., *Multiple negative-differential-resistance (MNDR) phenomena of a metal-insulator-semiconductor-insulator-metal (MISIM)-like structure with step-compositioned $In_xGa_{1-x}As$ quantum wells*, IEEE Trans. Electron Dev., **45**, pp.373-379, 1998.
6. BISWAS, S.K., SCHOWALTER, L.J., JUNG, Y.J., VIJAYARAGHAVAN, A., AJAYAN, P.M., VAJTAI, R., *Room-temperature resonant tunneling of electrons in carbon nanotube junction quantum wells*, Appl. Phys. Lett., **86**, pp. 183101, 2005.
7. BETHOUX, A.J.-M., HAPPY, H., SILIGARIS, A., DAMBRINE, G., BORGHETTI, J., DERYCKE, V., BOURGOIN, J.-P., *Active properties of carbon nanotube field-effect transistors deduced from S Parameters Measurements*, IEEE Trans. Nanotechnology, **5**, pp.335-342, 2006.
8. GEIM, A.K., NOVOSELOV, K.S., *The rise of graphene*, Nature Materials, **6**, pp. 181-183, 2007.
9. DRAGOMAN, D., DRAGOMAN, M., *Negative differential resistance of electrons in graphene barrier*, Appl. Phys. Lett., **90**, pp. 143111/1-3, 2007.
10. ECHTERMEYER, T.J., LEMME, M. C., BAUS. M., SZAFRANEK, B.N., GEIM, A.K., KURZ, H., *Nonvolatile switching in graphene field-effect devices*, IEEE Trans. Electron Devices, **29**,pp. 952-954, 2008.
11. MERIC, I., HAN, M.Y.,YOUNG, A.F., OZYILMAZ, B., KIM, P., SHEPARD, K.L., Current saturation in zero-bandgap, top-gated graphene field-effect transistors, Nature Nanotechnology, **3**, pp. 1-5, 2008.

Received October 10, 2008